SciencePG
Science Publishing Group

Design of an Experimental Rig for Testing Multipurpose Blades

Bala Gambo Jahun[1], Fati Adamu Astapawa[2], Balogun Shuaibu Alani[3]

[1]Department of Agricultural and Bioresource Engineering Abubakar Tafawa Balewa University, Bauchi, Nigeria

[2]Department of Agricultural and Environmental Engineering, Modibbo Adama University of Technology, Yola, Nigeria

[3]Department of Mechanical Engineering, Federal Polytechnic, Bauchi, Nigeria

Email address:

bgjahun@yahoo.com (B. G. Jahun)

Abstract: The design of experimental rig for testing multipurpose blades was done to come up with a good blade that would be suitable for the pulverization of oil palm fronds and reduce toque, noise and vibration and fuel consumption during field operations. A good consideration on the strength of soil and fronds was done during the design. Mild steel was chosen for the frame design. From the design, work done to till the soil was found to be 34785.5Nm, diameter of the shaft was calculated to be 30mm, power transmitted by the belt and pulley is 104.4KN which falls between 20-150Kw and belt type D was selected. Belt length was 1,071.3mm which is within the standard length of 3127mm and belt D3127-IS: 2494 was selected. The electric motor to drive the blades carrier considering the power transmitted a 3Hp was selected and a gear motor to drive the experimental rig 4Hp was selected. It is expected that it would guide the manufacturers and stake holders in the oil palm industry to adopt better tractor mounted Mulcher for discarding oil palm fronds waste.

Keywords: Experimental Rig, Blades, Crop Residues, Fronds, Mulching

1. Introduction

In recent years, there has been an increasing concerned in having zero emission and with recent implementation of environmental policies by the government and increasing awareness of the benefits and importance of soil organic matter in sustaining crop production, agro-industrial wastes and crop residues are being returned to, or left in the field as soil ameliorants and sources of nutrients [1, 2]. The world's total annual production of OPW is estimated at about 184 million tonnes with about 5% annual increment [3]. The palm oil industry generates its wastes mainly in the form of lignocellulosic materials from the plantation and the palm oil milling processes. The extraction of 1 ton of crude palm oil (CPO) requires about 5 tonnes of fresh fruit bunches (FFB) which generates about 1.15 tonnes of EFB and 2.45 tonnes of palm oil mill effluents as residues [4]. The processing of an FFB (weighing 20-30 kg) generates about 20% of CPO, about 25% nuts (comprising about 5% kernels, 13% fibre and 7% shell) and about 23% EFB [5, 6]. These figures keep rising yearly as the demand for palm oil increases, and only

about 10% of the generated OPW is utilized with the remaining 90% creating environmental burdens as their current disposal methods are unsafe. However, approaches of this kind carry with them various well known limitations to the soil and the infrastructure in the farm estate. It has become imperative to design suitable blades which would be used in a Tractor Mounted Mulcher by testing the blades using Multiuse blades Experimental Rig.

Organic mulching is one effective and established way to conserve soil and water. Utilization of oil palm residues such as pruned oil palm fronds (OPF) and empty fruit bunches (EFB) as a mulching material is a common conservation practice in oil palm plantations especially on non-terraced hill slopes [7, 8]. The popularity of using oil palm residues as mulching material is that oil palm produce large amount of biomass that have to be reused to avoid large amount of waste. Malaysia's palm oil industry produced 43 million tons of biomass [9].

The purpose of a tillage tool is to manipulate (change, move, or form) a soil as required to achieve a desired soil condition. There are three important initial factors to be

considered in tillage tool design. This includes; initial soil condition, tool shape, and manner of tool movement as stated by [10]. They said that as a result of these three initial independent input factors, another two output factors would be generated, namely; the forces required for manipulating the soil and finally obtained the soil condition. All these five factors mentioned are directly connected to a tillage design. Among the initial three input factors, the designer has only complete control on the tool shape. The manner of the tool movement involves orientation of the tool, its path through the soil, and its speed along the path. For tools that travel in a straight line (i.e., not rotary or oscillating tools), the path is usually identified by merely specifying the depth and width of cut. Orientation of a tool with a particular shape may significantly affect both the soil manipulation and the forces. Most of the time, the linkage system used to position a tool and affects both depth of cut and orientation of the tool. When sufficient power is available, speed is the easiest design factor to vary. Increasing the speed generally increases draft but also affects soil movement and breakup.

Draft required during tillage is a function of soil properties, working depth, tool geometry, travel speed, and width of the implement. It is an important parameter for measuring and evaluating implement performance for energy requirements [11]. Several studies have been conducted to measure draft and energy requirements of tillage implements under various soil conditions [12]. Soil properties that contribute to tillage energy are moisture content, bulk density, cone index, soil texture, and soil strength.

One of the criteria used to assess the suitability of a tool for soil manipulation is the force required in dragging the tool through the soil [13-17]. The interaction between tillage tools and soil is of a primary concern to the design and use of these tools for soil manipulation [18]. The draft required for a given implement will also be affected by the soil conditions and the geometry of the tillage implements [15, 16, 19]. Hence, the soil-tool-tillage combination should be studied for a given location and tool geometry to optimize the tool performance and energy efficiency. A tillage tool, particularly the blade system, must pulverize the soil and mix it well with the oil palm residue to the desire degree and manipulate the soil sufficiently. The energy applied to the soil by the blades must be exploited efficiently in incorporating the crop residue into the soil. The power requirement per unit of soil tilled with the crop residue must be low. The capacity of the blade system must be high as reported by [20]. The soil parameters used to determine the performance of tillage blades are soil toss, soil volume disturbed, depth of penetration of the blades and soil condition.

2. Materials and Methods

A special experimental rig primarily consisting of a blade carrier suitable for mounting blades that operates vertically of different shapes was designed as shown in Figure 1. The experiment requires testing of four different blades and picked the best among the blades borne in mind the torque, rate of pulverization, stress and strain on the blades, effective field capacity and fuel consumption. The overall size of the experimental rig was 2.4 x 1.2 x 3m with a weight of 1.5KN excluding the weight of the blades. The main frame is made of angle bar of 40 x 40mm with thickness of 2mm was used to support the load. The blades are to be mounted on the blade carrier of 590mm diameter having two holes were the blades are attached. The two holes were machined into round shapes. The blades would be fitted to the blade carrier with the aid of nuts and bolt and tightened firmly. An electric motor and a pulley were used to vary the speeds at 1000, 2000 and 3000 rpm. A dynamometer, a graduated ruler, stress strain gauges and fuel meter would be used to pull the data in the field.

In the working process, due to the advance movement of the equipment and the rotation movement of the rotor, the active parts penetrate into the soil and pulverize the oil palm crop residues with a particular shape of the blades in attachment. Under the action of centrifugal force, the soil slices are thrown over and mixes the residues with the soil at a depth of 30mm. As a result, the soil would be left behind the rotary rig in a loosened and mixed layer.

Proper calculation was done to avoid overload, and motor burn due to wrong estimation about load. The power transmission of the machine is by pulley and belt arrangement as shown in Figure 1. The speed of the blade carrier depends on:

   i. The speed of the electric motor.
  ii. The diameter of the pulleys.

The selected motor of 3hp delivers at speed of 1750 rpm which was connected to the pulleys. A diameter of the motor shaft pulley of 30mm was selected.

2.1. Parts of the Experimental Rig

The Experimental Rig is made up of the following units: the frame, electric motor, pulley, belt, chain and sprocket, driving wheel, disc plate, bevel gear, gear motor, bearing and coupler (Figure 1) and list of part is shown in Table 1 below.
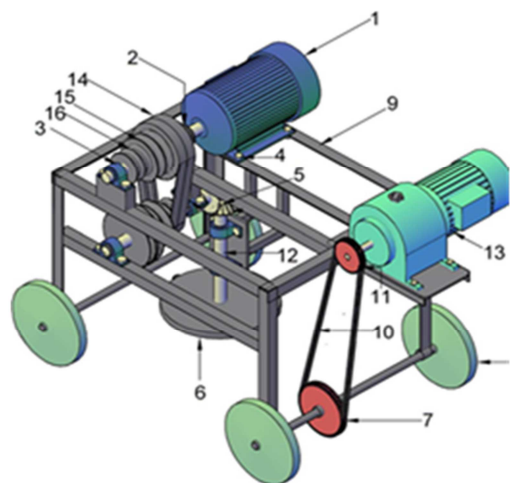

Figure 1. *Diagram of the Experimental Rig*

S/No	PART	QTY	SPECIFICATION
1	Electric Motor	1	3 Phase 3HP
2.	Coupling	1	D30x6mm, 60x6mm
3	Bearing	2	30x50mm
4.	Bolt/Nut	1	M12x50mm
5.	Bevel Gear	1	ID60x60, D30x60mm
6.	Disc Plate	1	OD570x19x50mm
7.	Gear	1	D200mmx50teeth
8.	Driving Wheel	4	D300x75mm
9.	Frame	1	50x50x5mm
10.	Chain Drive	1	Ø100mm
11.	Driving Sprocket	1	Ø100mmx30teeth
12.	Shaft	2	30x150mm 25x400mm
13.	Gear Motor	1	4HP, 100rpm
14	Belt	1	Ø300mm
15.	Large pulley	1	Ø210mm
16.	Small Pulley	1	Ø90mm

2.1.1. Electric Motor

Electric motor is the one of common device for rotating equipment and it is useful for smooth operation and makes our process faster and more efficient. 3Hp motor capacity and Speed of 1000, 2000 and 3000 rpm was considered for the load and speed.

2.1.2. Gear Motor

Gear motors are complete motive force systems consisting of an electric motor and a reduction gear train integrated into one easy-to-mount and -configure package. The reduction gear trains used in gear motors are designed to reduce the output speed while increasing the torque. The increase in torque is inversely proportional to the reduction in speed. Reduction gearing allows small electric motors to move large driven loads, although more slowly than larger electric motors. A 4Hp is used to drive the whole experimental Rig during operation.

2.2. Design Calculations

When analyzing a rotating system there are many calculations involved and a lot of assumptions made. This publication shows how the experimental rig was designed and methods considered. In designing a disc for machinery applications in soil and machinery dynamics, factors ought to be discussed as playing an important role like vibrations, thermal fatigue, analysis of blades etc. The starting point however, in rotating disc is always stresses due to inertia and these were primarily considered here.

2.2.1. Design of Disc

$$W_D = \frac{1}{2}\tau_s \times \pi \times Db \times \pi D \times z \qquad (1)$$

Where;

W_D = Workdone to till the ground

τ_s = Shear strength of soil

D = diameter of disc

b = thickness of blade

z = factor of safety = 5

$$W_D = \frac{1}{2}\times 350 \times 10^3 \times \pi \times 0.59 \times 0.003 \times \pi \times 0.59 \times 5 = 34785.5N_m$$

The power of the disc must be equal to the work to actualize tilling. Based on the equation above, the improved vibration response levels of discs rely on geometrically and physically accurate bladed disc models [22].

$$T = FR \qquad (2)$$

Where;

T = Torque

F = force

R = speeds

$$1.13 \times 10^3 \times \frac{0.59}{2} = 332.2N_m$$

2.2.2. Determination of Disc Thickness

Increasing the thickness of the disc will make it stronger and less susceptible to bending or breaking,

$$X = \frac{2F}{D\sigma_s} \qquad (3)$$

Where;

X = thickness of disc

σ = tensile strength of disc material

$$X = \frac{2 \times 1.13 \times 10^3}{0.59 \times 55 \times 10^3} = 0.1mm$$

3mm was chosen for flexural rigidity

2.2.3. Design of Shaft for Disc

A shaft is a rotating member, usually of circular cross section (either solid or hollow), transmitting power. It is supported by bearings and support gears, sprockets, wheels, rotors and is subjected to torsion and to transverse or axial loads, acting singly or in combination [21].

Using ASME CODE

$$d = \sqrt[3]{\frac{16}{\pi\tau_s}\sqrt{(k_b m_b)^2 + (k_t T)^2}} \qquad (4)$$

Where;

d = diameter of shaft, mm

k_b = combined shock and fatique factor applied to bending moment

k_t = combined shock and fatique factor applied to torsional moment

T = Torque, N/m

m_b = bending moment

τ_s = torsional shear stress

$$d = \sqrt[3]{\frac{16}{\pi \times 205 \times 10^6}\sqrt{(1.5 \times 176.1)^2 + (1 \times 332.2)^2}}$$

d = 22mm

30mm was chosen as the diameter of the shaft

2.2.4. Design of Shaft Based on Torsional Rigidity

Shafts are designed on the basis of torsional rigidity considerations. The total angle of twist θ in degrees is given by the Eq. (5). The permissible angle of twist or limiting value of twist for line shaft applications are 3° and 0.25° per m length of shaft respectively [23].

$$d = \sqrt[4]{\frac{584TL}{G\theta}} \qquad (5)$$

Where;

d = diameter of shaft, mm

T = applied torque, N/m

L = shaft length, mm

G = shear modulus of elasticity of the shaft material, N/m^2

θ = angle of twist (radians)

$$d = \sqrt[4]{\frac{584 \times 332.2 \times 0.53}{100 \times 10^9 \times 0.3}}$$

d = 43mm

45mm was chosen as the diameter of the shaft

2.2.5. Design of Shaft Based on Critical Speed

All rotating shaft, even in the absence of external load, deflect during rotation. The combined weight of a shaft and wheel can cause deflection that will create resonant vibration at certain speeds, known as Critical Speed. The Rayleigh-Ritz equation was used as in Eq. 6 which stated that maximum speed must not exceed 75% of critical speed [24]. Critical speed depends upon the magnitude or location of the load or load carried by the shaft, the length of the shaft, its diameter and the kind of bearing support.

$$N_c = \frac{30}{\pi}\sqrt{\frac{g}{\delta_{max}}} \qquad (6)$$

Where;

N_c = critical speed

δ_{max} = maximum deflection

For safety of operation let the speed equal to 75% of critical speed

$$d = \sqrt{\frac{100\pi}{0.7 \times 9.5 \times 78302.3}}$$

d = 25mm

30mm was chosen as the diameter of the shaft

2.2.6. Design of Bevel Gear

Torque application to a spiral bevel gear mesh induces tangential, radial, and separating loads on the gear teeth. For simplicity, these loads are assumed to act as point loads applied at the mid-point of the face width of the gear tooth. The radial and separating loads are dependent upon the direction of rotation and hand of spiral, in addition to

pressure angle, spiral angle and pitch angle. For transmitting motion between two perpendicular but coplanar shafts bevel gear were chosen [21].

I. Number of teeth

$$\eta_T = \frac{48}{\sqrt{1 + (V.R)^2}} \qquad (7)$$

Where;

V.R = velocity ratio

η_T = 32

36 teeth was chosen

II. Determination of Weight of Gears

As typified by [25], the procedure consists of five basic steps: definition of gear geometry, calculation of applied loads, resolution of the loads into each structural member, sizing of required member cross-sectional areas, and calculation of component and total structural weight. These steps were considered in determination of the gears weight.

$$W_g = \rho Vg = 7850 \times \frac{\pi}{3} \times \left[R^2H - r^2h\right]g \qquad (8)$$

Where;

W_g = weight

ρ = density

V = velocity m/s

g = acceleration due to gravity

$$W_g = 7850 \times \frac{\pi}{3}\left[0.053^2 \times 0.038 - 0.039^2 \times 0.026\right] \times 9.81$$

$$W_g = 6.4N$$

2.3. Bearing Selection

Each bearing should be selected according to the technical characteristics required by the specific application. Since the largest diameter obtained from the design is 45mm bearing number 209 was considered being the bore is 45mm.

2.3.1. Dynamic Radial Load

The choice of the appropriate type of bearing (radial, angular contact or thrust) is determined by the direction of the load which will act on the bearing. These bearings can accommodate a certain amount of axial load in addition to the radial load as its major advantage.

$$W = xVW_R + yW_A \qquad (9)$$

Where;

W_R = radial load, N

W_A = axial or thrust load, N

x = radial load factor

y = axial load factor

V = velocity factor

$$W = (0.56 \times 1 \times 1.13 \times 10^3) + 3 \times 134.6$$

$$W = 1.04 KN$$

2.3.2. Design of Basic Dynamic Radial Load Capacity

$$W_D = W \times K_s \qquad (10)$$

W_D = basic dynamic radial load capacity

K_s = service factor = 2 for mocerate shock load

$$W_D = (1.04 \times 2)$$

$$W_D = 2.08 KN$$

The dynamic and static basic capacities of bearing No. 209 are 25.5 and 18.3 respectively; therefore bearing number 209 is selected.

2.4. Selection of Belt and Pulley

Selecting the conveyor pulleys is started by specifying the belt tensions of the conveyor. Belt tensions come from the capacity calculations of the conveyor. Calculations can be made according to SFS-ISO5048.

$$\text{Power to be transmitted} = T\omega \qquad (11)$$

P = torque transmitted, N/m

T = tension on the tight and slack side of the belt, N

ω = velocity of the belt, m/s

$$P = 332.2 \times \frac{2\pi N}{60}$$

$$P = 332.2 \times \frac{2\pi 3000}{60}$$

$$P = 104.4 KN$$

From the design manual, the recommended belt for power range of (20-150) Kw is D. Therefore, belt type D was selected.

2.4.1. Determination of the Belt Length

To obtain good driving strength and good belt life, the belt pretension should be 1 to 8%, based on hardness and length of the belt [27]. For selected belt length, center distance, belt number has been determined by using the following Eq. 12 below.

$$L = \pi(r_1 + r_2) + 2X + \frac{(r_1 - r_2)^2}{x} \qquad (12)$$

L = total length of the belt pulley, mm

r_1 and r_2 = radii of the larger and smaller pulleys

x = distance between the centres of two pulleys, mm

$$L = \pi \times 150 + 600 + \frac{2500}{300} = 1,071.3 mm$$

For belt D the smallest standard length is 3127mm and therefore belt D3127- IS: 2494 was selected.

2.4.2. Maximum Tension in Belt

$$T_{max} = \sigma \times a \qquad (13)$$

T_{max} = maximum tension in belt, N

σ = maximum safe stress

a = width of the belt, mm

$$T_{max} = 2 \times 10^6 \times 504 \times 10^{-4}$$

$$T_{max} = 1030 N$$

2.4.3. Pulley Diameter and Selection

It is important that pulley is of sufficient diameter and the belt of sufficient section to transmit the required horsepower to the designed experimental rig. The minimum pulley diameters of a belt conveyor installation will be determined by the design and layout, stresses and splicing method of the belt. Based on torsional moment taking factor of safety as 5, the working stress 82MP the pulley diameter was calculated using Eq. 14 below.

$$d = \sqrt[3]{\frac{16T}{\pi\tau}} \qquad (14)$$

$$d = \sqrt[3]{\frac{16 \times 332.2}{\pi \times 82}}$$

d = 27mm

50mm was selected

For the small pulley, velocity ratio of 1: 2

$$\frac{N_1}{N_2} = \frac{1}{2} = \frac{D_2}{D_1} \qquad (15)$$

N_1 = shaft speed in rev/minute

N_2 = driven pulley speed in rev/minute

D_1 = diameter of the driving pulley, mm

D_2 = diameter of the driven pulley, mm

$D_1 = 2D_2 = 100 mm$

2.5. Design of Middle Shaft

Weight of pulley and the volume of pulley are approximated by the following formula.

$$W = \frac{\pi}{3}\left[R^2 H - r^2 h\right] \qquad (16)$$

$$W = \frac{\pi}{3}\left[58^2 \times 230 - 33^2 \times 100\right]$$

$$W = 7 \times 10^{-4} m^3$$

$$\text{Weight} = \rho v g \qquad (17)$$

Where;

ρ = density

v = velocity, m/s

g = acceleration due to gravity

$$\text{Weight} = 7850 \times 7 \times 10^{-4} \times 9.81 = 54 N$$

2.5.1. Determination of Shaft Diameter Based on ASME CODE

The shaft diameter can be calculated in terms of external loads and material properties. However, the below equation is further standarised for steel shafting in terms of allowable design stress and load factors in ASME design code for shaft.

$$d = \sqrt[3]{\frac{16}{\pi\tau_s}}\sqrt{(k_b m_b)^2 + (k_t T)^2} \tag{18}$$

Where;

d = diameter of shaft, mm

k_b = combined shock and fatigue factor applied to bending moment

k_t = combined shock and fatigue factor applied to torsional moment

T = Torque, N/m

m_b = bending moment

τ_s = torsional shear stress

$$d = \sqrt[3]{\frac{16}{\pi \times 205 \times 10^6}}\sqrt{(1.5 \times 126.5)^2 + (1 \times 332.2)^2}$$

d = 21mm

30mm was chosen

2.5.2. Determination of Shaft Diameter Based on Torsional Rigidity

$$d = \sqrt[4]{\frac{584TL}{G\theta}} \tag{19}$$

Where;

d = diameter of shaft, mm

T = applied torque, N/m

L = shaft length, mm

G = shear modulus of elasticity of the shaft material, N/m²

θ = angle of twist (radians)

$$d = \sqrt[4]{\frac{584 \times 332.2 \times 0.53}{100 \times 10^9 \times 0.3}}$$

d = 43mm

45mm was chosen

2.6. Selection of Electric Motor

Considering the power to be transmitted and to determine the appropriate electric motor for the experimental rig Eq. 20 was applied below.

$$P = (T_1 - T_2)V \tag{20}$$

Where;

P = power transmitted

T_1 = tension on the tight side

T_2 = tension on the slack side

V = velocity of the belt in m/s

T_c = centrifugal tension acting tangentially

$T_c = mV^2$

For belt type D m = 5.96N / m

$$V = \frac{\pi DN}{60} \tag{21}$$

D = diameter for the pulley shaft, mm

N = speed of pulley in rpm

V = 2.6m / s

P = (989.7 − 267.5) × 2.6

$$P_{hp} = \frac{1878}{750} = 2.5Hp$$

3Hp was selected

Power required driving the Shaft

$$P = T\omega \tag{22}$$

$$P = 1200 \times \frac{2 \times \pi N}{60}$$

$$P = \frac{1200 \times 2 \times \pi \times 50}{60}$$

$$P = 3142Nm / s$$

4Hp was chosen

2.7. Blades Shapes and Design

Four different blades were design (with different lifting angle of 90°, 120°, 60° and curved which serves as control) and develop with CAD methods like 3D modeling and analysis was used. Accordingly at the initial stage 3D Modeling was done on the basis of geometrical parameters normally which are similar to a commercially available blades using 3D CAD software. This model was analyzed through Solid Works for Finite Element Analysis particularly to investigate the main causes of wear and deformation as shown in Fig 2 below.
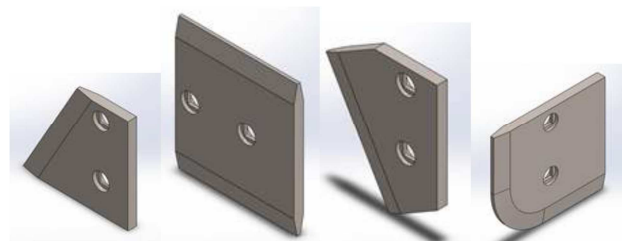

Figure 2. *Different Blades with lifting angles of 60°, 90°, 120° and Curved.*

3. Conclusion

The design and development of Multiuse laboratory blades testing experimental rig has been described. Appropriate design consideration and procedures have been taken into

account to ensure the robustness of the machine. What finally counts is the performance of the product, not a good figure of some kind especially since there are a lot of failure conditions that are unpredictable by calculations. Nevertheless, accurate analyzes are necessary to compare different designs and to create a robust product that fulfills the customers´ demands.

The dispensation of oil palm fronds will be enhanced to achieve the cleaner environment, improve soil nutrient and control soil erosion on relatively large scale for domestic and industrial uses.

It will guide the manufacturers and stake holders to modify the components of the existing machine which entails promotion of technology transfer and adoption for the pulverization of oil palm residues.

It is expected that the patronage by peasant farmers and other users of the new machine so modified will reduce extremely the labour, drudgery and cost involved in steering the Tractor mounted Mulcher for making it a user friendly.

Agricultural sector in Malaysia and other parts of the world where palm trees are grown will be enhanced once again through the use of such modified machines aimed at adding values to the present Mulcher used by the farmers.

The economy of Malaysia will be enhanced since embracing of such implement will help in clean environment and rich soil that would increase oil palm production, easy accessibility during replanting period and eradicate breeding ground of the Rhinoceros Beetle, a serious pest for oil palm plantations.

Acknowledgements

References

[1] Bundy, L., T. Andraski, and R. Wolkowski, *Nitrogen credits in soybean-corn crop sequences on three soils.* Agronomy journal, 1993. 85(5): p. 1061-1067.

[2] Rembon, F. and A. MacKenzie, *Soybean nitrogen contribution to corn and residual nitrate under conventional tillage and no-till.* Canadian journal of soil science, 1997. 77(4): p. 543-551.

[3] Shuit, S. H., et al., *Oil palm biomass as a sustainable energy source: a Malaysian case study.* Energy, 2009. 34(9): p. 1225-1235.

[4] Corley, R. and P. Tinker, *The palm oil.* World Agriculture Series, 2003.

[5] Corley, R. H. V. and P. Tinker, *The oil palm.* 2008: John Wiley & Sons.

[6] Yusoff, S., *Renewable energy from palm oil–innovation on effective utilization of waste.* Journal of cleaner production, 2006. 14(1): p. 87-93.

[7] Anderson, J. M., *Eco-friendly approaches to sustainable palm oil production.* J. Oil Palm Res., 2008: p. 127-142.

[8] Moradi, A., et al., *Effect of four soil and water conservation practices on soil physical processes in a non-terraced oil palm plantation.* Soil and Tillage Research, 2015. 145: p. 62-71.

[9] Chang, S. H., *An overview of empty fruit bunch from oil palm as feedstock for bio-oil production.* Biomass and Bioenergy, 2014. 62: p. 174-181.

[10] Abubakar, M. S. and Shittu, S. K, *Determination of Physical and Mechanical Properties of a soil related to the Design of Tillage Implement.* Proceedings of the 33rd National Conference and Annual General Meeting of the Nigerian Institution of Agricultural Engineers, 2012 33: p. 41-49.

[11] Chandon, K. and R. Kushwaha. *Soil forces on deep tillage tools.* in *The AIC 2002 Meeting CSAE/SCGR program Saskatoon, Saskatchewan, Canada July.* 2002.

[12] Grisso, R., M. Yasin, and M. Kocher, *Tillage implement forces operating in silty clay loam.* Transactions of the ASAE, 1996. 39(6): p. 1977-1982.

[13] McLaughlin, N., et al., *Energy inputs for conservation and conventional primary tillage implements in a clay loam soil.* Transactions of the ASABE, 2008. 51(4): p. 1153-1163.

[14] Naderloo, L., et al., *Tillage depth and forward speed effects on draft of three primary tillage implements in clay loam soil.* Journal of Food, Agriculture and Environment, 2009. 76(3): p. 382-385.

[15] Olatunji, O. and R. Davies, *Effect of weight and draught on the performance of disc plough on sandy-loam soil.* Research Journal of Applied Sciences, Engineering and Technology, 2009. 1(1): p. 22-26.

[16] Gill, W. R. and G. E. V. Berg, *Soil dynamics in tillage and traction.* 1967: Agricultural Research Service, US Department of Agriculture.

[17] Shen, J. and R. L. Kushwaha, *Soil-machine interactions: a finite element perspective.* 1998: Marcel Dekker Inc.

[18] Taniguchi, T., et al., *Draft and Soil Manipulation by Amoldboard Plow under Different Forward Speed and Body Attachments.* Transactions of the ASAE, 1999. 42(6): p. 1517.

[19] Yadav, B., I. Mani, and J. Panwar, *Design of tool carrier for tillage studies of disc in field conditions.* AGRICULTURAL MECHANIZATION IN ASIA AFRICA AND LATIN AMERICA, 2007. 38(2): p. 29.

[20] Khurmi, R. and J. Gupta, *Theory of machines.* 2005: S. Chand.

[21] Chan, Y. J., *Variability of blade vibration in mistuned bladed discs.* 2009, Department of Mechanical Engineering, Imperial College London.

[22] Naunheimer, H., et al., *Automotive transmissions: fundamentals, selection, design and application.* 2010: Springer Science & Business Media.

[23] Prabhakar, S., A. Sekhar, and A. Mohanty, *Transient lateral analysis of a slant-cracked rotor passing through its flexural critical speed.* Mechanism and machine theory, 2002. 37(9): p. 1007-1020.

[24] Kawalec, A., J. Wiktor, and D. Ceglarek, *Comparative analysis of tooth-root strength using ISO and AGMA standards in spur and helical gears with FEM-based verification.* Journal of Mechanical Design, 2006. 128(5): p. 1141-1158.

[25] Allen, S., Alfred, RH, and Herman, GL, *Machine Design.* Tata McGraw-Hill Publishing company Ltd. New Delhi, 2004 p. 101-127.

[26] Good, C. A., D. C. Viano, and J. L. Ronsky, *Biomechanics of volunteers subject to loading by a motorized shoulder belt tensioner.* Spine, 2008. 33(8): p. E225-E235.